SUPPORTING INFORMATION

AUTO-CATALYZED CROSSLINKING FOR NEXT-GENERATION OLED-DESIGN

By Daniel Volz, Thomas Baumann*, Harald Flügge, Mathias Mydlak, Tobias Grab, Michael Bächle, Christopher Barner-Kowollik* and Stefan Bräse*

TABLE OF CONTENTS

EXPERIMENTAL SECTION: GENERAL INFORMATION

^{1}H NMR spectra were recorded on a Bruker AM 400 (400 MHz) spectrometer as solutions in $CDCl_3$. Chemical shifts are expressed in parts per million (ppm) downfield from tetramethylsilane (TMS) and are referenced to $CHCl_3$ (7.26 ppm) as internal standard. All coupling constants are absolute values and J values are expressed in hertz (Hz). The description of signals include: s = singlet, bs = broad singlet, d = doublet, t = triplet, m = multiplet. The spectra were analyzed according to first order. The signal abbreviations include: Ar-H = aromatic proton; ^{13}C NMR spectra were recorded on a Bruker AM 400 (100 MHz) spectrometer as solutions in $CDCl_3$. The signals were allocated through DEPT-technology (DEPT = Distortionless Enhancement by Polarization Transfer). The signal abbreviations include: C-Ar = aromatic carbon, + = primary or tertiary carbon atom, − = secondary carbon atom, C_{quart} = quaternary carbon atom; MS (EI) (electron impact mass spectrometry) and HRMS (high resolution mass spectrometry): Finnigan MAT 90 (70 eV). The molecular fragments are quoted as the relation between mass and charge (m/z), the intensities as a percentaged value relative to the intensity of the base signal (100%). The abbreviation [M+] refers to the molecular ion.

FAB spectra were measured in 3-Nitrobenzylalcohol as matrix. The spectra of the complexes showed cluster ions of copper iodide and the ligands, having the general formula $[Cu_nI_{n-1}(ligand)_m]$+. The abbreviation [L] refers to the ligands in this context. Descriptions without nominated temperature were done at room temperature (rt), and the following abbreviations were used: calc. (theoretical value), found (measured value). Information is given in mass percent.

IR (infrared spectroscopy): FT-IR Bruker IFS 88. IR spectra of solids were recorded in KBr, and as thin films on KBr for oils and liquids. The deposit of the absorption band was given in wave numbers in cm-1. The forms and intensities of the bands were characterized as follows: s = strong 10–40% T, m = medium 40–70% T, w = weak 70–90% T, vw = very weak 90–100% T, br = broad.

Routine monitoring of reactions were performed using Silica gel coated aluminium plates (Merck, silica gel 60, F254), which were analyzed under UV-light at 254 nm and/or dipped in a solution of molybdato phosphate (5% phosphor molybdic acid in ethanol) and potassium permanganate (0.45 g potassium permanganate and 2.35 g of sodium carbonate in 90 ml of water) and heated with a heat gun.

Gel permeation chromatography was performed on a Polymer Laboratories (Varian) PL-GPC 50 Plus Integrated System, comprising an autosampler, a PLgel 5 µm bead-size guard column (50 × 7.5 mm), one PLgel 5 µm Mixed E column (300 × 7.5 mm) three PLgel 5 µm Mixed C columns (300 x 7.5 mm) and a differential refractive index detector using THF as the eluent at 35 °C with a flow rate of 1 mL min-1. The SEC system was calibrated using linear poly (styrene) standards ranging from 160 to 6 x 106 g mol-1 and linear poly (methyl methacrylate) standards ranging from 700 to $2{\cdot}10^6$ g mol^{-1}.

High Performance Liquid Chromatography was performed on a Agilent 1100 system with Waters C18 column, 4.60 x 75 mm, 3 µm loading as solid phase and water/methanol as a liquid phase at 45 °C with 2 mL min-1 flow rate and a linear solvent gradient from 90/10 MeOH/water at t = 0 min to 50/50 at t = 7 min.

Atomic absorption spectroscopy: To measure the copper content, samples (3 – 10 mg) were dried for 48 hours in vacuum, treated with nitric acid at 90 °C for one hour and transferred into volumetric flasks (100 mL). The flasks were filled with diluted nitric acid and aliquots were taken. An AAnalyst 200 (Perkin Elmer) with a HKL Cu Lumina lamp at 324.8 nm was used. From the concentration of the aliquots, the copper content of the samples was calculated. Due to this elaborate preparation of the aliquots, we assumed that the error of this method is +/– 1.8 %.

Synthetic procedures and analysis of the products: The used synthetic strategy is shown in **Scheme 1** in the main text and **Scheme S1** herein. Solvent mixtures are understood as volume/volume. Solid materials were powdered. All solvents, reagents and chemicals were purchased from Sigma Aldrich, Fluka, Lanxess and Merck. All reactions involving moisture sensitive reactants were carried out under an argon atmosphere using oven dried and/or flame dried glassware. Vinylbenzylchloride and styrene were passed over activated alumina prior to use. AIBN was recrystallized from methanol. All other solvents, reagents and chemicals were used as purchased unless stated otherwise.

EXPERIMENTAL SECTION: SYNTHESIS OF THE POLYMERS

The synthetic strategy used for the current work is summarized in **Scheme 1** in the main text. To synthesize the alkyne-substituted PyrPHOS-complex **1**, a variation of a previously reported method was employed. Complex **1** was prepared in three steps with an acceptable overall yield of 50%. The synthetic scheme for the polymer is given in **Scheme S1.**

The base azide-polymer was prepared with a living polymerization protocol enabling a good control of chain length, end-groups and molar-mass dispersity Đ_M. (**Scheme S1** and **Table S1**) Four polymers **2a-d** having various chain lengths ranging from 1 000 Da to 27 000 Da and the corresponding Click-polymers **3a-d** by reaction with complex **1** in dichloromethane were prepared. The synthesis of a homopolymeric poly-(vinylbenzylazide) has not been successful: The direct polymerization of vinylbenzylazide gave an insoluble, yellow foam. Elemental analysis showed a much smaller nitrogen percentage than expected, leading us to the conclusion that during the radical-involving process, the azides decompose by formation of nitrogen. The homopolymerization of vinylbenzylazide showed little control of the molar-mass dispersity Đ_M. However, as shown in **Table S1**, we could achieve good control of the mass distribution and the end groups by copolymerization of vinylbenzylazide with styrene. As expected, the mild substitution of chloride with azide did change the SEC-result only slightly due to some influence of the hydrodynamic radius. The end groups remained intact as confirmed by elemental analysis (sulfur) and ^{1}H NMR-spectroscopy in good agreement with the literature. Four polymers **2a-d** having various chain lengths ranging from 1 000 Da to 27 000 Da and the according Click-polymers **3a-d** by reaction with complex **1** in dichloromethane were prepared.

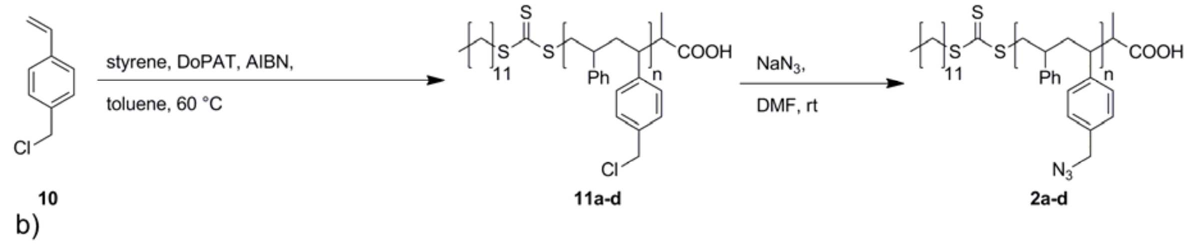

Scheme S1. Synthesis of azide polymers **2a-d.**

EXPERIMENTAL SECTION: SYNTHETIC PROCEDURES

General procedure of RAFT polymerization: Vinylbenzylchloride **8** (5 mL, 35 mmol) and styrene (5 mL, 43 mmol) were put in a Schlenk-tube equipped with a stirring bar. The appropriate amount of initiation-solution and dry toluene were added to reach a total volume of 15 mL. The mixture was flushed with dry nitrogen for 30 minutes. The flask was subsequently placed into a pre-heated bath at 60 °C. After 24 hours, the contents of the flask were slowly poured into 300 mL of ice cold methanol. The white-to-yellow precipitate was filtrated, washed with 50 mL of cold methanol and 50 mL of pentane and dried in vacuum.
The stock-solution consisted of 370 mg of DoPAT and 35 mg of AIBN (molar ratio 5/1) in 5 mL of dry toluene. The solution was stored at -30 °C and consumed within 72 hours after preparation. The optimized concentrations and reaction times for **10a-d** are summarized in **Table S1**.

General procedure of substituting chloride with azide: The polymer (1.00 g, ca. 3.5 mmol, calculated by skipping the end-groups) and sodium azide (1.00 g, 15.38 mmol) were dissolved in 20 mL of dry DMF. The reaction was stirred for 24 h at room temperature. After this time, the whole mixture was added into 500 mL of brine, the white precipitate was filtrated, washed with 100 mL of water, 200 mL of methanol and 50 mL of pentane, subsequently. The polymer was dissolved in dichloromethane, filtered over a 0.45 µm-disc-filter and precipitated again from methanol. The product was dried in vacuum.

General procedure for the attachment of a copper complex to an azide-substituted polymer: Equimolar amounts of the alkyne-substituted complex and the azide-substituted polymer (calculated according to the number of alkyne-containing ligands attached to the complex) were weighted in a flask equipped with a stirring bar and dissolved in dichloromethane (10 mL per 1 g of complex). The mixture is stirred at room temperature for 24 hours, the precipitated product was filtered off and washed with 50 mL of pentane, methanol and dichloromethane, subsequently. The product was dried under vacuum.

Remark: ^{31}P-spectra of ligands and complexes.
^{31}P-NMR-spectra of Cu(I)-phosphane-complexes are known to be very sensitive regarding geometric variations of the molecular structure. Even in solid state ^{31}P-NMR-spectra, the occurrence of two different conformers can result in doubled signal sets, as it was shown e.g. by Healy and coworkers in 1989.[1] In solution, similar processes as above, e.g. less hindered rotatability of the P-bound substituents as well as other dynamic mechanism like dissociation and rearrangements often lead to one broad phosphorus resonance, even if a complex contains crystallographically non-equivalent P-ligands in solid state. This seems to be the case for all the complexes analyzed in this study as it was not possible to resolve any of the three different P-signals expected for a hypothetical, rigid complex. In any case, broad signals were found. Crespo et al. rationalized this phenomenon for two related structure (**Figure S1**). [2] While the chelated ligands in complex A give one sharp resonance in ^{31}P-NMR, substitution of the acetonitrile ligands with two more equivalents of the same dipyridylphenylphosphane—ligands as non-chelating ligands, only one broad signal was observed. The cause of this broadening is most likely a more dynamic behavior of the complex in solution.

Figure S1. Only very rigid Cu(I)-phosphane complexes show sharp signals in 31P-NMR (complex A), while flexible structures often lead to broadened signals. (see: reference [2])

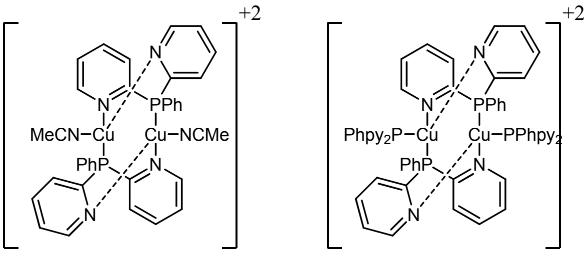

Complex **A:** sharp signal
Complex **B:** broad signal

4-Methyl-2-(diphenylphosphino)-pyridine **6**.

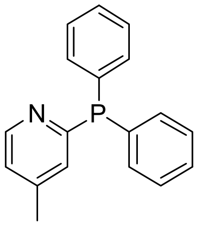

Lithium (764 mg, 110 mmol, 2.20 equiv.) was suspended in 100 mL THF under nitrogen. Chlorodiphenylphosphine (10.59 g, 50 mmol, 1.00 equiv.) was added dropwise at 0 °C and the reaction mixture was allowed to stir at room temperature over night giving a red solution of lithium diphenylphosphine. A solution of 2-chloropicoline (6.38 g, 50 mmol, 1.00 equiv.) **5** in 10 mL dry THF was added dropwise at 0 °C. The resulting brownish solution was stirred at room-temperature. After completion of the reaction, the excess of lithium diphenylphosphine was quenched with 3 mL of water. The mixture was evaporated and filtered over Celite with cyclohexane/ethyl acetate = 1/1. The solvent was removed and the resulting white solid was used without further purification. (11.36 g, 41 mmol, 82%). – R_f = 0.81 (CH/EE, 1/1) – ^{1}H NMR (400 MHz, $CHCl_3$): δ = 2.10 (s, 3 H, $\mathbf{CH}_3$), 6.95-6.85 (m, 1 H, Ar-H), 7.10–7.30 (m, 11H, Ar-H), 8.52–8.55 (m, 1 H, 3-H) ppm. – ^{31}P-NMR (101 MHz, $CHCl_3$): δ = −3 ppm. – IR (DRIFT): ν = 3299 (w), 3051 (w), 2925 (w), 2117 (vw), 1957 (vw), 1814 (vw), 1586 (s), 1548 (m), 1478 (m), 1433 (s) ν (P-Ph), 1386 (m), 1093 (vw), 1027 (vw), 988 (vw), 827 (vw), 743 (s), 696 (s), 504 (m) cm^{-1}. – MS (70 eV, EI), *m/z* (%): 277 (2) [M$^+$], 200 (1) [M$^+$–Ph], 164 (61), 130 (100), 103 (17), 84 (55), 77 (17) [Ph$^+$], 56 (54), 39 (33). – HR-EIMS ($C_{18}H_{16}NP$): calc. 277.1020; found 277.1022.

4-(But-3-yn-1-yl)-2-(diphenylphosphino)-pyridine **7**.

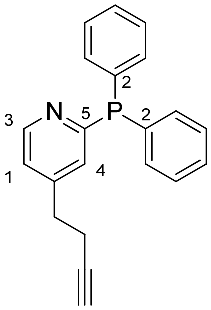

(4-Methylpyridyl)-diphenylphosphine **6** (8.31 g, 30 mmol, 1 equiv.) was dissolved in 80 mL of dry THF and cooled to −78 °C under nitrogen. Lithiumdiisopropylamide (1.8 M solution in THF, 20 mL, 36 mmol, 1.20 equiv.) was added dropwise resulting in a dark-brownish solution. The cooling bath was removed and the reaction mixture was allowed to stir for 2 hours. The mixture was cooled to −78°C again and propargylbromide (80% in toluene, 4.0 mL, 36 mmol, 1.20 equiv.) was added slowly. After 30 minutes, the cooling bath was removed and the mixture was stirred over night at room temperature. The mixture was quenched with 4 mL of water, the solvent was evaporated and the product was purified with column chromatography (eluent cyclohexane/ethyl acetate = 5/1). The product was dried in vacuum resulting in a brown oil. (5.86 g, 19 mmol, 62%) – R_f = 0.45 (CH/EE 5/1) – ^{1}H NMR (400 MHz, $CHCl_3$): δ = 2.10 (s, 1 H, $CH_2CH_2CC\mathbf{H}$), 2.23 (t, ^3J = 7.6 Hz, 2 H $CH_2C\mathbf{H}_2CCH$), 2.51 (t, ^3J = 7.6 Hz, 2 H $C\mathbf{H}_2CH_2CCH$), 6.90 (m, 1 H, 4-H), 7.10–7.30 (m, 11H, Ar-H), 8.52 (m, 1 H, 3-H) ppm. – ^{13}C NMR (100 MHz, $CHCl_3$): δ = 19.34 (–, $CH_2\mathbf{C}H_2CCH$), 33.8 (–, $\mathbf{C}H_2CH_2CCH$), 69.8 (+, $CH_2CH_2C\mathbf{C}H$), 82.6 (+, $CH_2CH_2\mathbf{C}CH$), 122.4 (+, C-1), 129.0 (+, CH_{arom}), 134.8 (C_{quart}, C-2), 136.4 (+, C-3), 150.2 (C_{quart}, C-4), 164.0 (C_{quart}, C-5) ppm. – IR (ATR): ν = 3258 (s) ν(CCH), 3051 (m), 2930 (m), 2117 (vw), 1735 (vw), 1586 (vs), 1547 (vs), 1478 (m), 1454 (m), 1434 (vs) ν(P-Ph), 1386 (s), 1308 (w), 1278 (w), 1188 (w), 1158 (w), 1121 (w), 1093 (m), 1069 (w), 1027 (m), 988 (m), 830 (w), 743 (vs), 696 (vs), 640 (s), 546 (m), 504 (m), 455 (m), 425 (w) cm^{-1}. – MS (70 eV, EI), *m/z* (%): 315 (19) [M^+], 276 (60) [M–Propargyl$^+$], 199 (21), 183 (21), 164 (47), 130 (93), 77 (22) [Ph^+], 43 (100). – HR-EIMS ($C_{21}H_{18}NP$): calc. 315.1177; found 315.1173.

Tris-(4-but-3-yn-1-yl-2-diphenylphosphino-pyridine)-dicopper-diiodide **1**.

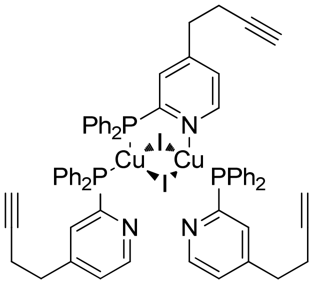

Butynyl-PyrPHOS **7** (473 mg, 1.5 mmol, 1.5 equiv.) and copper iodide (191 mg, 1 mmol, 1 equiv.) were suspended in 10 mL dichloromethane in a dark flask and stirred until the copper iodide dissolved. The resulting yellowish solution was filtered over a 0.45 µm-disc-filter and the product was precipitated from hexane resulting in a light green solid. (1220 mg, 0.91 mmol, 91%). – ^{1}H NMR (250 MHz, $CHCl_3$): δ = 1.80 (d, ^4J = 4.0 Hz, 1 H, $CH_2CH_2CC\mathbf{H}$), 2.23 (dt, ^3J = 7.6 Hz, ^4J = 5.0 Hz, 2 H $CH_2C\mathbf{H}_2CCH$), 2.51 (t, ^3J = 7.6 Hz, 2 H $C\mathbf{H}_2CH_2CCH$), 6.90–7.60 (m, 12H, Ar-H), 8.42–8.52 (m, 1 H, Ar-H) ppm. – IR (ATR): ν = 3294 (w) ν(CCH)), 3048 (w), 2923 (w), 1587 (m), 1547 (m), 1479 (m), 1434 (m) ν(P-Ph), 1388 (m), 1094 (m), 989 (m), 853 (m), 744 (s), 694 (vs) $\delta_r(CH_2)$, 636 (s), 507 (s), 468 (s), 436 (m) cm^{-1}. – MS (FAB, NBA), m/z (%): 1454 (1) [$Cu_5I_4L_2^+$], 1389 (3) [$Cu_4I_4L_2^+$], 1264 (2) [$Cu_4I_3L_2^+$], 1199 (6) [$Cu_3I_3L_2^+$], 1074 (14) [$Cu_3I_2L_2^+$], 1010 (1) [$Cu_2I_2L_2^+$], 883 (53) [$Cu_2IL_2^+$], 760 (8) [$Cu_3I_2L^+$], 693 (45) [$Cu_2I_2L^+$], 568 (60) [Cu_2IL^+], 378 (78) [CuL^+], 316 [L^+] (17), 154 (100), 127 (63) [I^+]. – $C_{63}H_{48}Cu_2I_2N_3P_3$ + 0.5 CH_2Cl_2 (1367.0): calc. C 55.69 H 4.05, N 3.07 Cu 9.28; found C 55.17, H 3.99, N 2.83 Cu 10.18. (EA contains 0.5 molecules of dichloromethane in the crystal)

Tris-(4-(2-(1-benzyl-1H-1,2,3-triazole-4-yl)ethyl)-2-(diphenylphosphino)-pyridine)-dicopper-diiodide **4**

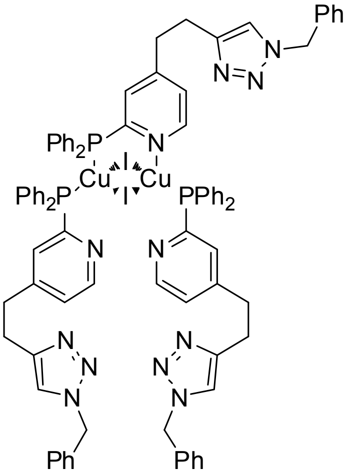

Synthesis according to the general procedure gave **4** in quantitative yield as a yellowish solid. – ^{1}H NMR (250 MHz, $CHCl_3$): δ = 2.88 (m, 4 H, Pyr$C\mathbf{H}_2C\mathbf{H}_2$), 5.49 (s, 2 H, Ph$C\mathbf{H}_2$), 7.10–7.60 (m, 17 H, Ar-H), 7.82–7.84 (m, 1 H, Ar-H), 8.78–8.80 (m, 1 H, Ar-H) ppm. – ^{31}P-NMR (101 MHz, CHCl3): δ = −7 ppm. – IR (ATR): ν = 3043 (vw), 2920 (w), 2850 (vw), 1620 (vw), 1596 (vw), 1504 (vs), 1467 (m), 1450 (m), 1310 (m), 1267 (m), 1227 (s), 1180 (w), 1104 (w), 1055 (w), 1016 (w), 940 (vw), 824 (w), 793 (m), 765 (m), 745 (m), 721 (s), 635 (vw), 624 (w), 578 (vw), 561 (m), 521 (w), 464 (vw), 420 (w) cm^{-1}. – MS (FAB, 3NBA), m/z (%): 1977 (1) [$Cu_4I_4L_3^+$], 1913 (1) [$Cu_3I_4L_3^+$], 1789 (3) [$Cu_3I_3L_3^+$], 1657 [$Cu_4I_4L_2^+$], 1531 [$Cu_4I_3L_2^+$], 1466 [$Cu_3I_3L_2^+$], 1341 (6) [$Cu_3I_2L_2^+$], 1276 (1) [$Cu_2I_2L_2^+$], 1214 (1) [$Cu_3I_1L_2^+$], 1149 (3) [$Cu_2IL_2^+$], 892 (3) [$Cu_3I_2L^+$], 701 (10) [Cu_2IL^+], 449 (4) [L+H$^+$], 154 (100), 127 (86) [I^+]. – EA ($C_{84}H_{75}Cu_2I_2N_{12}P_3$, 1726.40): calc. C 58.44, H 4.38, N 9.74 Cu 7.36; found. C 58.44, H 3.81, N 7.72 Cu 7.10.

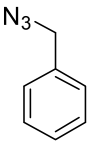

Benzylazide. According to [ref 8]. Benzylbromide (11.97 g, 70 mmol, 1.00 equiv.) was dissolved in 50 mL DMF and sodium azide (5.85 g, 90 mmol, 1.30 Äquiv.) was added. The excess of sodium azide was removed by filtration and 70 mL of dichloromethane was added to the mixture. The solution was washed with brine (3 × 100 mL) and dried over magnesium sulfate. Removal of the solvent gave benzylazide as a yellow oil. (7.46 g, 56 mmol, 80%). – ^{1}H NMR (400 MHz, $CHCl_3$): δ = 4.39 (s, 2 H, $\mathbf{CH_2}N_3$), 7.48-7.52 (m, 5 H, Ar-H) – IR (ATR): ν = 3443 (vw), 3065 (w), 3033 (w), 2931 (vw), 2877 (vw), 2096 (vs) ν= (N_3), 1605 (vw), 1496 (w), 1454 (m), 1350 (m), 1256 (m), 1202 (w), 1078 (vw), 1029 (vw), 877 (w), 750 699 (w), 569 (w) cm^{-1}. – MS (70 eV, EI), *m/z* (%): 133 (47) [M^+], 118 (32), 104 (50) [M^+ - N_2], 91 (100) [M^+ - N_3], 77 (85) [M^+–CH_2N_3], 65 (17), 51 (35), 39 (13). – HR-EIMS ($C_7H_7N_3$): calc. 133.0638; found 133.0637.

Remark: While the ^{1}H NMR- and IR-spectra for the polymers **11a-d**, **2a-d** and **3a-d** were the same for different chain lengths, the exact elemental composition was not, as expected. At this point, full data is given for **11a**, **2a** and **3a**. More data of $Đ_M$, chain length and the reaction conditions can be found in **Table S1**. To calculate the elemental composition for the polymers, we calculated the theoretical values without the endgroups. The values for sulfur were in the range of the detection limit and tended to aberrate slightly. However, they remained constant before and after the introduction of the azide and dropped to approximately half of their value after the Click-reaction, as expected.

Poly-(styrene)-co-(vinylbenzylchloride) **11a**.

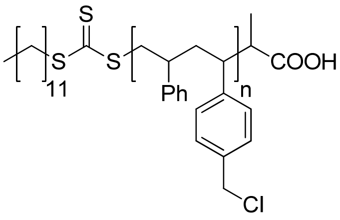

Prepared according to the general procedure. The ratio of styrene versus vinylbenzylazide in the product was determined with ^{1}H NMR-spectroscopy as 52 to 48. – ^{1}H NMR (250 MHz, CHCl$_3$): δ = 0.90–1.05 ($\mathbf{CH_3}$ of $\mathbf{CH_3}$CHCOOH and $\mathbf{CH_3}$C$_{11}$H$_{22}$), 1.14–1.25 ($\mathbf{CH_2}$ of CH$_3$C$_{11}\mathbf{H_{22}}$), 1.26–2.50 ($\mathbf{CH_2}$, **CH** of polymer backbone and CH$_3$**CH**COOH), 4.35-4.60 (CH**2**Cl) 6.20–7.30 (m, Ar-H) ppm. – IR (DRIFT): ν = 3025 (vw), 2920 (w), 1601 (vw), 1511 (vw), 1493 (w), 1451 (w), 1421 (vw), 1265 (w), 1182 (vw), 1111 (vw), 1020 (vw), 909 (vw), 824 (w), 760 (w), 699 (vs), 674 (m), 542 (w) cm^{-1}. – EA ($C_{17}H_{17}Cl$): calculated C 79.52 H 6.67; found C 77.73 H 6.46 S 0.62. (calculated without regarding the end groups) – M$_n$ 7 600 Da, Đ$_M$ 1.09.

Poly-(styrene)-co-(vinylbenzylazide) **2a**.
Prepared according to the general procedure. – ^{1}H NMR (250 MHz, CHCl$_3$): δ = 0.90–1.05 ($\mathbf{CH_3}$ of $\mathbf{CH_3}$CHCOOH and $\mathbf{CH_3}$C$_{11}$H$_{22}$), 1.14–1.25 ($\mathbf{CH_2}$ of CH$_3$C$_{11}\mathbf{H_{22}}$), 1.26–2.50 ($\mathbf{CH_2}$, **CH** of polymer backbone and CH$_3$**CH**COOH), 4.15-4.40 (CH**2**N$_3$) 6.20–7.30 (m, Ar-H) ppm. –– IR (DRIFT): ν = 3025 (w), 2920 (w), 2848 (w), 2091 (vs) ν= (N$_3$), 1775 (vw), 1601 (vw), 1511 (vw), 1493 (w), 1451 (w), 1421 (vw), 1340 (w), 1246 (m), 1204 (w), 1111 (vw), 1020 (vw), 965 (vw), 877 (w), 843 (w), (15 (m), 760 (m), 699 (vs), 561 (m) cm^{-1}. – EA ($C_{17}H_{17}N_3$): calculated C 77.54 H 6.51 N 15.96 S 0.00; found C 76.14 H 6.35 N 15.92 S 0.62. (calculated without regarding the end groups) – M$_n$ 6 700 Da, Đ$_M$ 1.16.

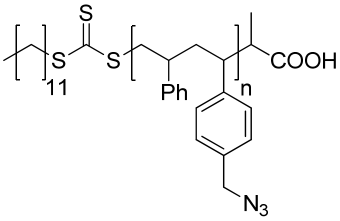

Poly-(4-(2-(1-4-vinylbenzyl-1H-1,2,3-triazol-4-yl)ethyl)-2-(diphenylphosphino)-pyridine)-co-styrene) @ CuI **3a**.
The complex polymer **3a** was synthesized according to the general procedure in 97% yield – IR (DRIFT): ν = 3023 (vw), 2917 (vw), 2848 (vw), 2089 (vw) residue of ν= (N$_3$), 1769 (w), 1587 (vw), 1545 (vw), 1507 (vw) 1480 (vw), 1450 (vw), 1434 (vw), 1387 (vw), 1364 (vw), 1221 (m), 1190 (m), 1161 (m), 1121 (w), 1095 (w), 1080 (w), 1048 (w), 1015 (w), 829 (w), 742 (w), 692 (vs), 546 (w), 500 (w), 464 (w), 436 (w), 407 (vw) cm^{-1}. – EA ($C_{114}H_{105}Cu_2I_2N_3P_3$): calculated. C 64.68 H 5.00 Cu 6.00 N 7.96 S 0.00; found C 63.53 H 5.14 N 6.54 S 0.26. (calculated without regarding the end groups)

Table S1. Overview: results of the reactions giving **11a-d** and **2a-d** and the corresponding reaction conditions for the polymerizations as well as the substitution of chloride with azide.

	stage	ĐM	Mn [g mol-1]	concentration DoPAT* [mmol l-1]	reaction time [h]
11a	chloride	1.09	7 590	70.0	24
11b	chloride	1.12	10 300	35.0	24
11c	chloride	1.27	17 770	3.5	24
11d	chloride	1.29	27 500	3.5	36
2a	azide	1.16	6 960	-	24
2b	azide	1.20	11 200	-	24
2c	azide	1.24	16 070	-	24
2d	azide	1.27	30 370	-	24

---

* The ratio of AIBN/DoPAT was 1/5 for **11a-d.**

ATR-NIR-SPECTROSCOPY AND MECHANISTIC CONSIDERATIONS

The Click-reaction of complex **1** with benzylazide was monitored *in situ* with an ATR-NIR-spectrometer probe consisting of a Bruker Vertex 80 FT-IR/NIR Spectrometer with an InGaAs detectors, CaF_2 beam splitter, a 2 mm external probe (Hellmar), as well as an ATR unit. Specifically, the energy absorption at 6500 cm^{-1}, corresponding to the overtone-band of the alkyne-bond stretching mode, was quantified to track the extent of the reaction. In this reaction, complex **1** (0.6 M) was added to benzylazide (1.8 M) in dichloromethane, so that the alkyne and azide groups had equimolar concentrations. The reaction was allowed to proceed at ambient conditions. To derive the experimental standard deviation, spectra were collected every 30 seconds for 5 minutes for a 0.6 M solution of the alkyne-complex and the signal at 6500 cm^{-1} was integrated. The standard deviation of the measured integrals was determined to be 0.01993 and the initial value of the band (0 percent conversion) was found to be 0.59918. Given this, the relative values of the peak integral were determined, permitting the quantification of the conversion of the alkyne to the Click-product.

As indicated in **Figure 2** in the main text, the azide was added after five minutes to the solution of the complex, resulting in a slight decrease of the alkyne-concentration due to dilution. During a period of 40 minutes, the concentration of the alkyne fell below the experimental standard deviation indicating the completion of the reaction. When going from our model system **4** to the cross-linked polymer **3**, one has to keep in mind that it is highly unlikely to reach full conversion in this kind of reaction when using a polymeric azide. At some point, no free complex will be present in the reaction mixture, since the addition of even one of the three alkyne-moieties to the polymer backbone will disrupt the diffusion of the reactants towards each other to some extent.

As predictable from these considerations, we observed the characteristic stretching frequency of remaining free azide-groups in the product with ATR-IR-spectroscopy. Although the intensity decreased dramatically (over one order of magnitude relative to modes of the aryl styrene-frame at 3040 cm^{-1}), this proves that there are still some unreacted azide – and probably also alkyne – groups in the cross-linked product. Since the relative IR-intensity of the alkyne-group in the PyrPHOS-complex is much lower than the one of the azide-group in the polymer, it is comprehendible that we were not able to detect any trace of remaining alkyne in the infrared-spectra. Via elemental analysis of carbon, hydrogen, nitrogen, sulfur and copper, we were able to show that the composition of the product is indeed as expected for an atom economic addition of both reactants.

Even in more diluted solutions than we employed in our NIR-experiments, precipitation of complex-polymer **3** was observed after 30 minutes and less. Since theoretically, the reaction of the small molecule azide should be much faster than the polymeric one without the diffusion-hindrance of the attachment to a backbone, this early precipitate should feature a much higher azide-content than the product obtained after longer reaction times since the rate is probably slower. However, even at an earlier stage of the reaction, cross-linked polymers should be insoluble. Again, we checked the azide stretching-band at 2090 cm^{-1} with IR-spectroscopy and found that the relative intensity of this early-stage product is reduced to only 70% of the intensity of the azide-polymer. As a qualitative result, we can report that the rate of the Click-reaction is dependent on the length of the polymer. In general, it takes longer till the beginning of the precipitation of the first insoluble complex polymer when comparing higher chain lengths with lower ones. Since it was not possible to properly quantify this effect, it could not be proved whether this is truly due to a higher rate of the reaction with smaller polymers or simply a solubility effect: The concentration of linking knots per polymer chain is smaller for the longer chains if an equal velocity is assumed. This effect would correspond with a higher solubility for longer chains, so the precipitation would be delayed. After completion of the reaction (24 hours), there are no measurable differences in terms of IR-bands or elemental composition.

PHOTOPHYSICAL MEASUREMENTS

Sample-preparation and additional comments:

All solid samples were measured as powder samples. Soluble compounds were dissolved in dichloromethane and degased by flushing with dry nitrogen, respectively. Complexes **1** and **4** are soluble in solvents such as chloroform or dichlorobenzene, but of course, the cross-linked polymers **3a-d** are not. No photophysical differences between the four polymers could be identified. To avoid extensive repetition, only the product from the reaction of complex **1** and polymer **3a** are included. The emission maxima deviated in the range of only 1 nm, which is – considering the accuracy of the method – very constant. Full data for each emissive species analyzed in the present study, including CIE-coordinates and peak wavelengths are given in the main text (**Figure 3**)

Steady-state absorption, emission- and excitation spectra in both solution and solid (powder samples) were recorded with a Thermo Scientific (Evolution 201) UV-visible spectrophotometer and an Horiba Scientific FluoroMax-4 spectrofluorometer using a JX monochromator and a R928P PMT detector.

For quantum yield measurements, an absolute PL quantum yield measurement system from Hamamatsu Photonics was used. The system consisted of a photonic multichannel analyzer PMA-12, a model C99200-02G calibrated integrating sphere and a monochromatic light source L9799-02 (150 W Xe- and Hg-Xe-lamps). Data analysis was done with the PLQY measurement software U6039-05, provided by Hamamatsu Photonics.

Absorption spectra

Figure S2. Absorption spectra of the non-clicked complex **1**, small-molecule-complex **4** and free ligand **7** in dichloromethane solution. The relative absorbance of complex **4** is greatly enhanced due to the additional benzyltriazole-moieties. (Due to insolubility, complexes **3a-d** could not be analyzed with this method).

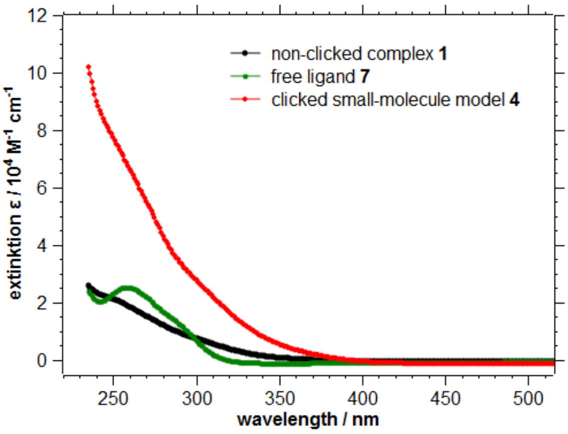

While the free ligand **7** shows a well structured spectrum (**Figure S2**) with a local maximum at 261 nm (ε = 2.53 10^4 M^{-1} cm^{-1}) and a additional shoulder at 290 nm (ε = 1.46 10^4 M^{-1} cm^{-1}), both complexes **1** and **4** are associated with rather unstructured spectra. This behavior is, however, common for copper(I) complexes and can also be found for other emissive Cu(I) compounds, according to the literature,[3] while, on the other hand, there exist other examples with more pronounced absorption structure.[4] Several broad, overlapping shoulders can be found in spectra of **1** and **4**, which were assigned as ligand centered for **1:** at 250 nm and 250 nm; for **4:** 265 nm, respectively. Charge transfer transitions were assigned for all shoulder with energies lower than 300 nm; for **1**: 300 nm and 330 nm; for **4**: 300 nm and 350 nm, respectively. Full data for the peak/shoulder-position, values for ε and possible transitions are collated in **Table S2**. It should be noted that the relative extinction of complex **4** is very significantly higher than for complex **1** because of the introduction of six non-conjugated, high-energy-absorbing chromophores through the Click-reaction (Three phenyl moieties and three triazole moieties per complex). Several charge transfer bands could be assigned for the complexes, ranging from 300 to 350 nm. The missing structure of the spectra can be explained with small energy separation between the absorbing transitions.

Table S2. Measured electronic absorption maxima and extinction coefficients of compounds **1**, **4** and **7**. (solution, dichloromethane)

Compound	$\lambda_{abs,}$[nm]	ε* [10^4 M^{-1} cm^{-1}]	possible transition
ligand **7**	261	2.53	LC, Ph, π-π*
	290 (sh)	1.5	LC
complex **1**	250 (sh)	2	LC, Ph, π-π*
	300 (sh)	0.8	(X+M)LCT
	330 (sh)	0.1	(X+M)LCT
complex **4**	250 (sh)	7.4	LC, Ph, π-π*
	265 (sh)	6.2	LC, Ph, π-π*
	300 (sh)	2.6	(X+M)LCT
	350 (sh)	0.5	(X+M)LCT

* = extinction coefficients are calculated relative to one equivalent of complex molecule. Since there are more than one equivalents of attached benzyltriazole-chromophores per molecule complex, these values have to be handled with care.

(sh) = shoulder. LC = ligand-centered transition. (X+M)LCT = halide and/or metal to ligand charge transfer-transistion. For the shoulders, approximate values are given.

Excitation and emission spectra in the solid state

Figure S3. Solid-state excitation spectra at ambient temperature. Before and after the Click-reaction, a very broad emission is evident. For these spectra, emission at 550 nm was observed.

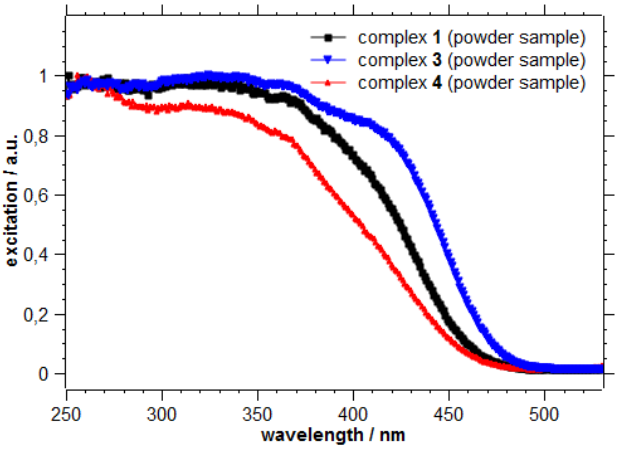

Solid state emission spectra are given in the main text (**Figure 3**), while excitation spectra are shown in **Figure S3**. The emission spectra are centered around 550 nm with unstructured, very broad emission bands (half-height-width: ca. 150 nm). Such broad spectra are fairly common for emissive Cu(I)-complexes and a result of the charge-transfer-character of the emissive transitions.[5,3,6,7] The emission spectra of **1**, **3a** and **4** are almost congruent, showing that the emission behavior is hardly disturbed by the Click reaction.

Such a behavior is reflected in the excitation spectra: Broad, ill structured bands ranging from 250 to 400 nm are found. While the edge of the excitation band is shifted slightly, there are - qualitatively- no mayor differences between the excitation profiles.

Excitation and emission spectra in solution

Figure S4. (left) Solution emission spectra at room temperature. For the Click product, an additional emission around 445 nm appears. This is a result of an incomplete intra- and intermolecular energy transfer from the benzyltriazole to the emitting complex. The excitation wavelength was 400 nm for both cases. (right) solution excitation spectra at room temperature. For both spectra, emission at 610 nm was observed. Since complex **4** showed two emission maxima, we also observed emission at 445 nm, which resulted in a similar, yet more structured peak at 360 nm. Due to insolubility, complexes **3a-d** could not be analyzed with this method.

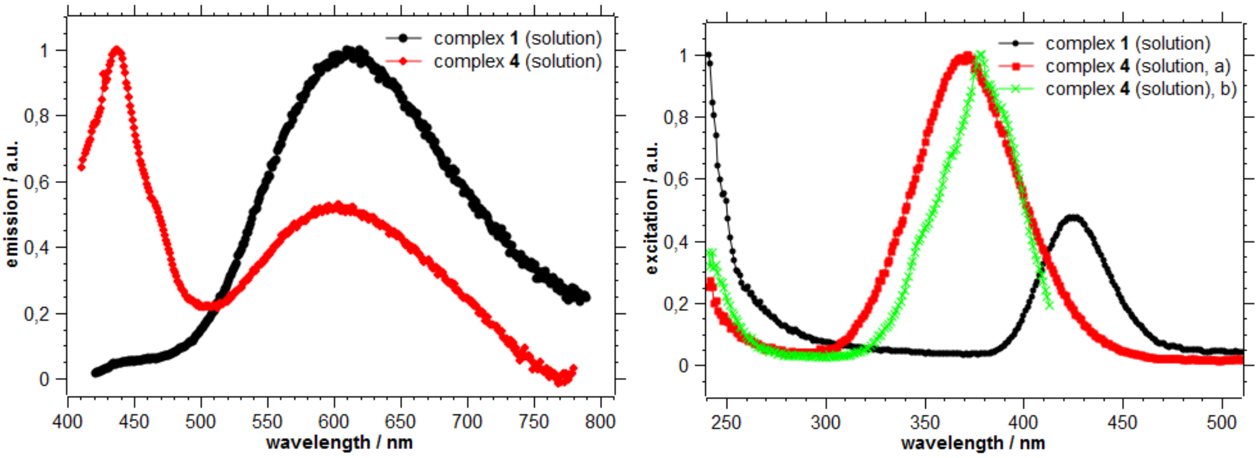

Excitation and emission spectra in dichloromethane are given in **Figure S4**. In both cases, broad, unstructured charge-transfer-emission bands are found in solution. The spectra show a red-shift of about 60 nm from 550 to 610 nm, probably due to a less rigid environment compared to the solid state. Since the life-time of the excited state is in the order of µs for Cu(I)-complexes,[5,8,3] a vibrational relaxation is expected in solution due to a higher degree of freedom. For the model compound **4**, an additional emission band appears by excitation at 400 nm, which is probably located on the benzyl-triazole-chromophor. This emission band is much slimmer, showing a fine structure consisting of two shoulders left and right to the maximum, as expected for a organic fluorescent dye.

In the excitation-scan, spectra are much slimmer compared to the solid-state. Comparision of complex **1** and **4** shows a shift to lower energies after the Click-process. For **4**, the spectra are much more structured, mirroring the two shoulders observable in the emission-scan. By observing the direct emission of the triazole-moieties at 445 nm (case b), the excitation spectra obtained turn even more structured. This seeming disagreement with the absorption spectra is due to the presence of the phenyl-rings from the ligands (PPh_2R), dominating the absorption spectra.

Excitation and emission spectra in a dichloromethane matrix at 77 K

Figure S5. (left) Emission spectra of complex **1** and **4** in dichloromethane matrix at 77 K. Both spectra show the same peak-position and –shape. The additional maximum at 445 nm (observable at room temperature for complex **4)** does not appear in the rigid low temperature matrix. Both samples were excited at 400 nm. (right) excitation spectra of complex **1** and **4** in dichloromethane matrix at 77 K. Both spectra show the same peak-position and –shape. Even at lower temperatures, broad excitation spectra are found.

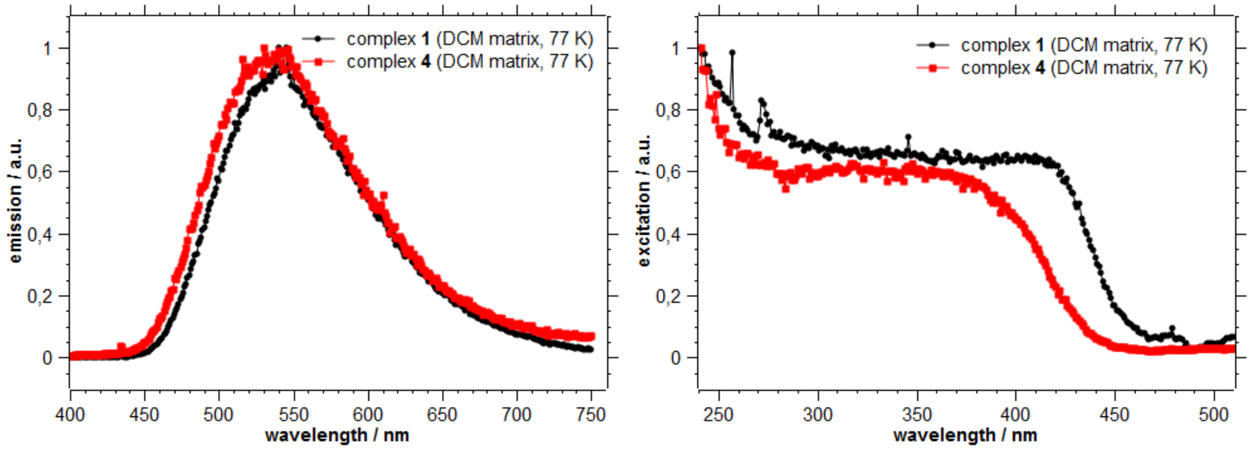

Even at lower temperatures (see **Figure S5**), the emission spectra are broad and unstructured. However, the band is slightly more slim; with a reduced half-peak bandwidth compared to the spectra measured at ambient temperature. Again, the spectra are congruent for the two complexes. Both spectra are shifted to higher energies, which is a relatively common behavior for Cu(I) complexes, which has been observed often upon cooling such substances.[3] The excitation spectra partly resemble the excitation spectra in solution (right half of the excitation band), since the shift between the edges is in the same order of magnitude than the shift between the isolated peak found in solution. However, the left part is –as it has been observed at room temperature- very broad, also ranging up to 250 nm.

THERMOGRAVIMETRIC ANALYSIS

Figure S6. Thermogravimetric analysis data for the range of 100 to 500 °C for complex polymer **3a** and the reactants, polymer **2a** and complex **3**.

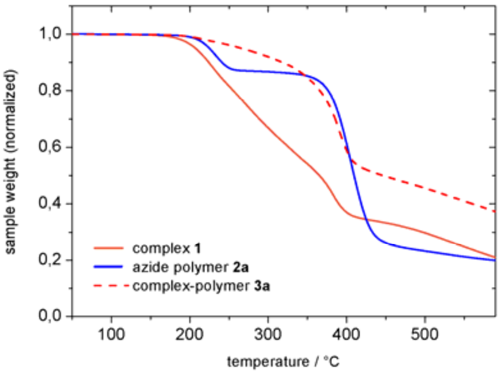

TGA was measured with a TGA Q5000 V3.10 Build 258 (TA Instruments) in a platinum pan with a constant heating rate of 5 °C/min to a maximum temperature of 700 °C. Both the sample gas (25 mL/min) and the balance gas (10 mL/min) were nitrogen. Sample amounts of approximately 1.5 mg were used. Thermal decomposition events were deduced by analyzing the maxima of the derivative of the TGA data. For complex **1** and as an example, polymer **2a** and **3a**, full data is shown in **Figure S6**.

As pointed out in **Table S3**, the stability of the complex polymers is enhanced drastically by 100 °C in comparison with both the non-linked complex **1** and the azide-polymers **2a-d**. Starting at 229 °C, complex **1** decomposes constantly upon further heating until a mass loss of over 65% at 400 °C. At 700 °C, a constant, inert residue, with 16% of the original mass of the sample remained. While the thermal degradation of complex **1** proceeds in a rather undefined way, the TGA-measurements of the azide-polymers **2a-d** gave more insight in the actual decomposition processes: At first, there is a process starting at around 230 °C with a defined mass loss of around 12%. This mass loss corresponds with the extrusion of N_2 from the azide moieties quite well.

Table S3. Thermogravimetric analysis and molar mass distribution of **2a-d** and **3a-d**.

	stage	$Đ_M$	M_n [g mol^{-1}]	decomposition (TGA)^1 [°C]
2a	azide	1.16	6 960	232, 406
2b	azide	1.20	11 200	229, 404
2c	azide	1.24	16 070	217, 399
2d	azide	1.27	30 370	213, 395
3a	complex	-	-	328, 404
3b	complex	-	-	334, 403
3c	complex	-	-	404^2
3d	complex	-	-	335, 408

1The alkyne-complex **1** shows two thermal decomposition reactions at 229 °C and at 383 °C. **2**The first decomposition event could only be observed as a shoulder of the latter reaction.

While the thermal degradation of complex **1** proceeds in a rather undefined way, the TGA-measurements of the azide-polymers **2a-d** gave more insight in the actual decomposition processes: At first, there is a process starting at around 230 °C with a defined mass loss of around 12%. This mass loss corresponds with the extrusion of N_2 from the azide moieties quite well. At circa 400 °C, there is another decomposition event leaving 17% of inert residue at 700 °C. For complex-polymer **3a**, TGA showed two ill resolved decomposition events at 335 and 409 °C with a remaining inert residue of around 28%. Interestingly, the thermal stability of these polymers seems to slightly decrease with growing chain length, as both thermal decomposition reactions shift to lower temperatures showing a maximal range of 19 °C. For the cross-linked polymers **3a-d**, the thermal stability rises around almost a hundred degrees, independently from the chain length of the polymers. As expected, the stability of the emitting material is enhanced by the cross-linking process.

DEVICE FABRICATION AND PROPERTIES

Figure S7. Schematic energy level diagram for the device: ITO/PEDOT:PSS (95 nm)/PTPB(xx nm)/$Cu_2PyrPHOS_3$:TPBi:PVK (30 nm)/TPBi (30 nm)/LiF (2nm)/Ag (70 nm). HOMO and LUMO values of the $Cu_2I_2PyrPHOS_3$ system are from cyclovoltammetry-measurements and were published recently.[9] Due to its insulating characteristics, the HOMO and LUMO energies of the polystyrene backbone were omitted for clarity. They are −7.0 eV for the HOMO and −3.2 eV for the LUMO, respectively.[10] All other frontier orbital energies were taken from published data.[11,12]

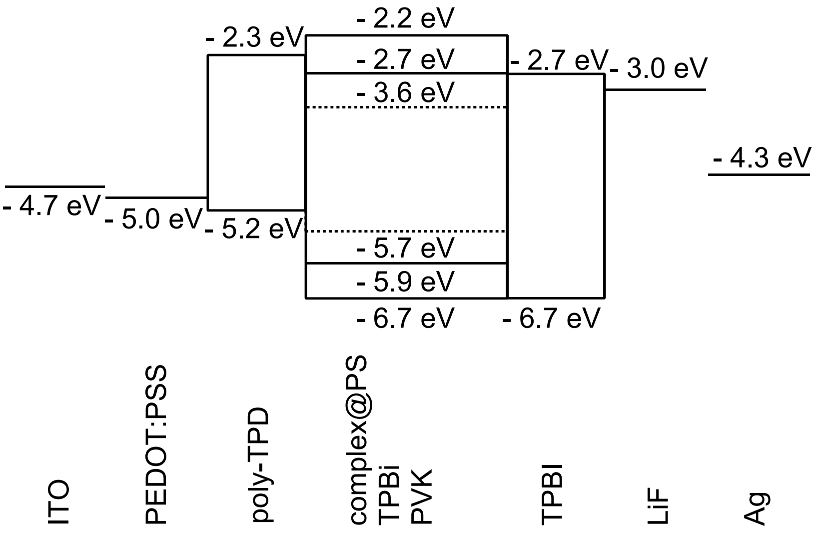

Figure S8. Poly-TPD ADS254BE was used as hole-transporting polymer. TPBi was used in the emitting layer and the electron-transporting layer. Poly-vinyl-carbazole (PVK) was used as an additive to prevent crystallization of TPBi.

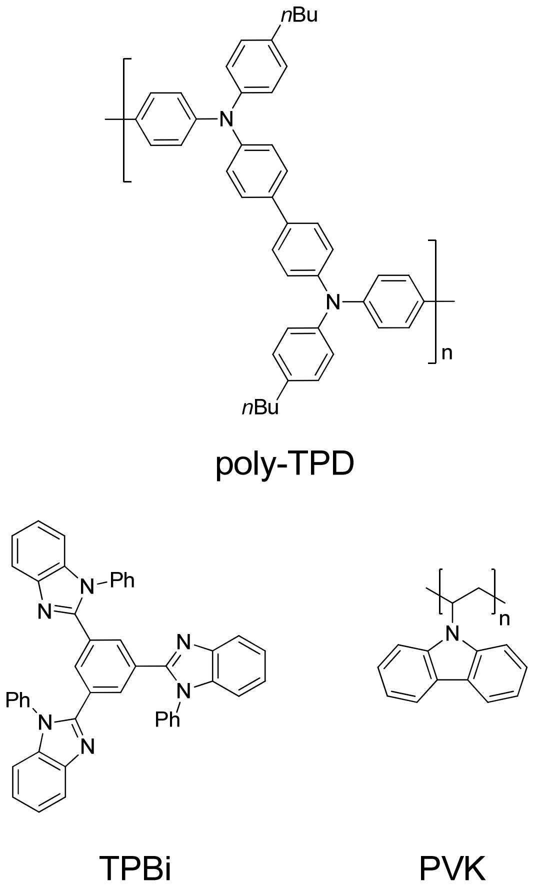

Materials. Poly-TPD was provided by American Dye Source (ADS254BE). PEDOT:PSS was provided from Heraeus (Al4043). All other chemicals and solvents used for device preparation were provided from Sigma-Aldrich and used as received.

Device preparation. Prior to the device preparation, the ITO coated glass substrates were cleaned by subsequent sonication in acetone and isopropanol for 15 minutes, followed by an UV ozone treatment for 10 min. The layer thickness of all spin-cast layers was determined with a thin film profiler by Veeco (Dektak 150). A 95 nm anode buffer layer of PEDOT:PSS was spin-cast on the ITO substrates and dried by baking the substrates at 120 °C for 30 minutes. The hole transporting layer (16 nm) was made by casting poly-TPD from chlorobenzene. The HTL was annealed at 120 °C for 30 minutes. The emitting layer consisted of 45% TPBi as an host material, 10% PVK to prevent crystallization and 45% of emitting material.

Complex **3a** was mixed with stoichiometric amounts of the crosslinking azide polymer **2a**, (device **Ia**) while complexes **1** (device **II**) and **4** (device **III**) were mixed with the same amount of non-functionalized polystyrene in order to introduce a similar amount of insulating material for better comparability of the devices. The layer thickness was 30 nm. The emitting layer was dried at 90 °C for one hour. 30 nm of TPBi was evaporated and the layer thickness was monitored by a quartz-crystal thickness/ratio monitor. For the device consisting of complex **3a**, 30 nm TPBi was spin-cast from toluene, additionally (device **Ib**). LiF (2nm) and Ag (70 nm) were evaporated successively. The devices were protected with an encapsulation foil provided by 3M. The pixel size was 25 mm^2. Except for the spin coating of the PEDOT-layer, all processes were carried out in the controlled atmosphere of a nitrogen glovebox. Physical characterization was carried out at ambient conditions at ambient temperature using a BoTest measurement unit. The devices were tested within 2h of fabrication.

Figure S9. L-I-V-curves for all devices prepared in this study.

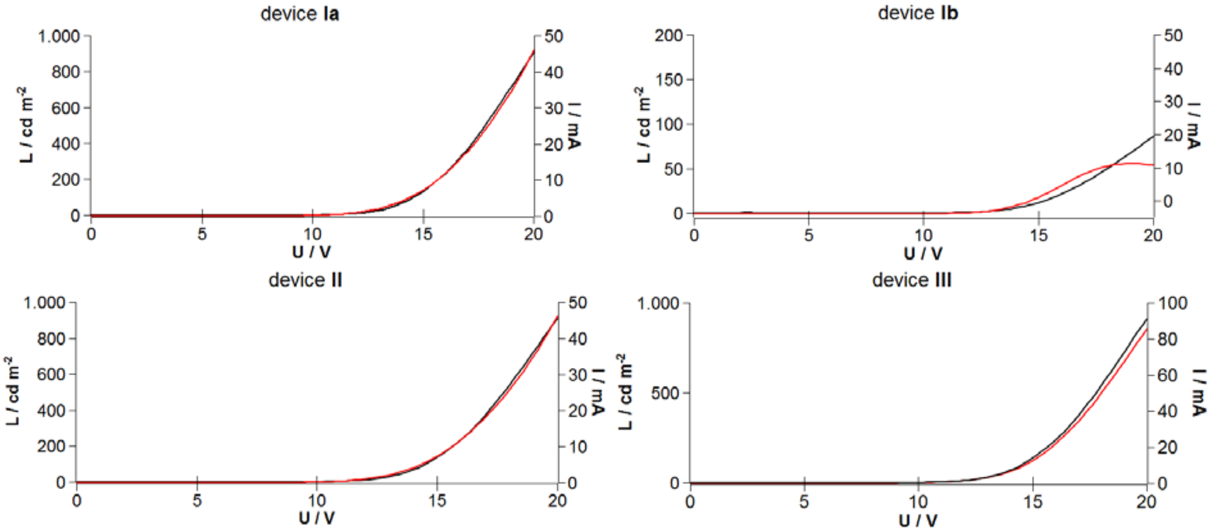

REFERENCES (SI)

1. P. Healy and J. Kildea, *Aust. J. Chem.*, 1989, **42**, 965.
2. O. Crespo, M. C. Gimeno, A. Laguna, and C. Larraz, *Z. Naturforsch.*, 2009, **64b**, 1525–1534.
3. R. Czerwieniec, J. Yu, and H. Yersin, *Inorg. Chem.*, 2011, **50**, 8293–301.
4. R. D. Costa, D. Tordera, E. Ortí, H. J. Bolink, J. Schönle, S. Graber, C. E. Housecroft, E. C. Constable, and J. a. Zampese, *J. Mater. Chem.*, 2011, 16108–16118.
5. Z. Liu, M. F. Qayyum, C. Wu, M. T. Whited, P. I. Djurovich, K. O. Hodgson, B. Hedman, E. I. Solomon, and M. E. Thompson, *J. Am. Chem. Soc.*, 2011, **133**, 3700–3.
6. D. M. Zink, T. Grab, T. Baumann, M. Nieger, E. C. Barnes, W. Klopper, and S. Bräse, *Organometallics*, 2011, **30**, 3275–3283.
7. N. Armaroli, G. Accorsi, F. Cardinali, and A. Lostorti, *Top. Curr. Chem.*, 2007, **280**, 69–115.
8. M. Hashimoto, S. Igawa, M. Yashima, I. Kawata, M. Hoshino, and M. Osawa, *J. Am. Chem. Soc.*, 2011, **133**, 10348–51.
9. D. M. Zink, M. Bächle, T. Baumann, M. Nieger, M. Kühn, C. Wang, W. Klopper, U. Monkowius, T. Hofbeck, H. Yersin, and S. Bräse, *Inorg. Chem.*, 2012, submitted.
10. C. Duke and T. Fabish, *Phys. Rev. Lett.*, 1976, **37**, 1075–1078.
11. Y. Tao, C. Yang, and J. Qin, *Chem. Soc. Rev.*, 2011, **40**, 2943–70.
12. Q. Sun, Y. A. Wang, L. S. Li, D. Wang, T. Zhu, J. Xu, C. Yang, and Y. Li, *Nature Photonics*, 2007, **1**, 717–722.